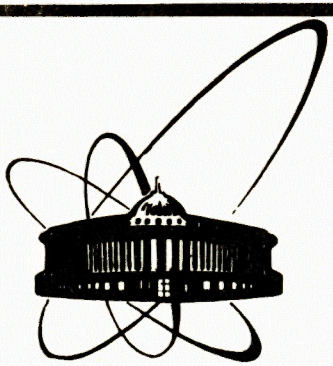

объединенный
институт
ядерных
исследований
дубна

E17-83-284

N.Angelescu, G.Nenciu, N.S.Tonchev

ON THE INFLUENCE OF THE RESERVOIR AND OF THE SHAPE OF THE FERMI SURFACE ON THE PHASE DIAGRAM OF THE TWO-BAND MODELS FOR Cr ALLOYS

Submitted to "Journal of Physics F : Metal Physics"

1983

1. INTRODUCTION

There exists a large body of theoretical work (see, e.g., references in the recent systematizing work by Buker[1]) trying to explain the itinerant antiferromagnetism of chromium alloys and their phase diagram. Below the Néel temperature, $T_N \approx 312^\circ K$, pure chromium exhibits an antiferromagnetic structure which can be characterised by a sinusoidal modulation of the spin density of wave vector, $\vec{Q} = \frac{1}{2}\vec{G} + \vec{q}$ ($\vec{G}$ is a reciprocal lattice vector), incommensurate ($\vec{q} \neq 0$) with respect to the lattice. The transition at T_N is of first order, as established by neutron diffraction[2], specific heat[3] and latent heat[4] studies. The magnitude of $\vec{q}$ is known to increase with lowering temperature below T_N[5,6].

When alloying Cr with small quantities of Mn, the Néel temperature increases but the qualitative picture does not change until a critical Mn concentration is attained. Above that concentration the transition at T_N becomes of second order into a commensurate ($\vec{q} = 0$) spin density wave (CSDW) phase and it is accompanied at a lower temperature, T_{CI}, by a first order transition from the CSDW phase into a sinusoidal incommensurate spin density wave (ISDW) phase[7]. The general belief is that the mechanism responsible for the appearance of the SDW is the strong correlation between the electrons in a band at the Γ point and the holes in a band at the H point[8,9]. The electron-hole correlation is favoured by the nearly perfect nesting of parts of the Fermi surfaces of the two bands, which in turn is controlled by the position of the Fermi level. It is accepted that alloying with Mn and V affects nothing but the electron-to-atom ratio. This justified the attempts, originating with Shibatani et al.[10] and Rice[11], to obtain the phase diagram of all Cr-Mn, V alloys starting from one Hamiltonian describing the electron-hole pairing (of the kind previously used by Keldysh and Kopaev[12] in connection with the transition into the excitonic insulator state); this Hamiltonian is supposed to contain the relevant part of the Coulomb interaction. The problem is further solved via a variational procedure.

Along this line of thought, a model is specified by:

a) the form of the energy spectra of the two interacting bands;
b) the kind of spatial dependence of the order parameter (e.g., single $\vec{Q}$-state, cubic state, etc.);

c) the power of the reservoir, i.e., the ratio of the density of states in the spectator (noninteracting) bands and that in the two interacting bands.

At a higher level of sophistication one takes into consideration different scattering mechanisms via finite electron lifetimes, magneto-strictive effects, etc.

It turned out that the above approach met only a limited success. In fact, in different works the models and their parameters are chosen so as to obtain (even semiquantitative) agreement with part of the experimental facts[1,13-17], but by now nobody succeeded in explaining all (be it qualitative) features of the phase diagram within one model, with parameter values in a reasonable agreement with actual facts. One cannot escape the feeling that, though the mechanism behind the phenomenon has been correctly guessed, some basic point has been missed. We already pointed out in two recent notes [18,19] that this missing point might be the proper use of the condition of conservation of the total electron number, wherever a finite reservoir power is considered in conjunction with a first order phase transition (as should be in the case of Cr).

In view of this, it is worth-while to reconsider the matter using the correct approach in Refs.[18],[19] and to clarify the ability of such mean field models to reproduce qualitatively the experimental facts. This is what we intend to do in the paper, restricting ourselves to the simplest situation of an infinite lifetime, when one has coalescing tricritical and Lifschitz points, so one can investigate locally the phase diagram via the Landau expansion. The ISDW state is supposed to be a single Q state, i.e., the spatially modulated order parameter (gap) is taken as:

$$\Delta(\vec{r}) = \Delta[\exp(i\vec{Q}\vec{r})\cos(\theta/4) + \exp(-i\vec{Q}\vec{r})\sin(\theta/4)], \qquad (1.1)$$

where Δ , θ and $q = |\vec{Q} - \frac{1}{2}\vec{G}|$ are real variational parameters, and the direction of $\vec{Q}$ is fixed along one of the axes. ($\theta = 0$ corresponds to a helical ISDW, $\theta = \pi$ to a sinusoidal ISDW). Thus, the only freedom left is the choice of the dispersion laws of the interacting bands and of the reservoir power, and we shall concentrate on their influence on the phase diagram around the triple point. It turns out that:

(i) The variation of the reservoir power does not change the order of the phase transitions, but strongly influences the positions of the phase boundaries; for reasonable reservoir powers (of an order of unity), one obtains with lowering temperature the correct sequences: P (i.e., paramagnet) - CSDW-ISDW for higher Mn concentration and P-ISDW for smaller Mn concentration or in Cr-V alloys;

(ii) Under the usual approximations and after suitably rescaling the variational parameters, the dispersion law enters only as the factor $\langle(\vec{v}_{\vec{k}} \cdot \vec{q})^4\rangle / \langle(\vec{v}_{\vec{k}} \cdot \vec{q})^2\rangle^2$ (where $\vec{v}_{\vec{k}}$ is the Fermi velocity at $\vec{k}$ and $\langle - \rangle$ denotes an average over the Fermi surface) into the coefficient of $q^4\Delta^2$ in the Landau expansion; see also Ref.[1]. This allows one to interpolate between the extreme cases of spherical and octahedral Fermi surfaces by varying this coefficient. The order of the P-ISDW transition depends on the value of the latter. As the unequal sphere model[11] gives a fairly strong first order transition (providing for reasonable reservoir power a wider region of mixed states than seems to be supported by experiment), while the octahedron model[10] gives a 2nd order transition, one can expect that working with actually realistic dispersion laws will provide the wanted weak 1st order P-ISDW transition. On the other hand, the CSDW-ISDW transition is of first order for both the unequal sphere and octahedron models and is in fact quite insensitive to the shape of the Fermi surface.

(iii) For a fixed Mn concentration smaller than the critical value, q increases with lowering temperature below T_N whenever the reservoir power is smaller than about 25,6 (the accepted values for Cr alloys safely satisfy this bound), irrespective of the shape of the Fermi surfaces. On the other hand, for strong reservoirs, q decreases with lowering temperature in the pure ISDW phase (as found also by Nakanishi and Maki [14] for the unequal sphere model with infinite reservoir).

Let us emphasize that we are concerned here with correctly solving a model, already proposed and currently used for describing Cr alloys. While, as discussed above, it is beyond doubt that the model with realistic parameter values is able to reproduce reasonably well the experimental facts, there is still a problem to be discussed related to the structure of the CSDW-ISDW and P-ISDW phase mixtures. Indeed, the model discards the long range part of the Coulomb interaction, what is expected to be a reasonable approximation only if the electron density is constant in space, because otherwise the Coulomb energy cost would be prohibitive. Hence only a mixed state like a homogeneous fluid of "quasi-particles" with two different energy spectra is consistent with the approximations. Therefore, if the mixed phases turn out experimentally to be macroscopically inhomogeneous*, one has to refine the model in order to obtain a reliable account of what actually happens in the temperature range corresponding now to the phase mixture. Refined

* Their very existence, at least for the CSDW-ISDW case, seems to be settled, see Geerken et al.[7], but we are not aware of results concerning their structure.

treatment is called for also by the existence of hystereses, which should be accounted for by metastable states.

In Sec.2 we shall formulate the model and write down the Landau expansion. Our further treatment consists in two steps:

1°. minimization of the trial thermodynamic potential with respect to Δ, θ and q at fixed μ, T, what is done in Sec.3;

2°. calculation of the Helmholtz free energy at a fixed total (i.e., in the interacting bands and in the finite reservoir) electron density via the Legendre transformation[20] of the optimal grand-canonical potential obtained in step 1°, what is done in Sec.4. The T-dependence of q is discussed in Sec.5. Finally, let us stress that, in all previous papers on Cr known to us, either one considers a fixed value of μ (infinite reservoir)[14], or, following Shibatani et al.[10] and Rice[11], one reverses the order of steps 1° and 2°, i.e., performs first the Legendre transformation (what, in view of the differentiability of the trial grand-canonical potential as a function of μ, is equivalent to solving the equation for the Fermi level shift) and only afterwards minimizes over $\Delta(\vec{r})$. As explained in detail in Refs.[18],[19], the result may change at reversing the order of steps 1° and 2°, and the correct result is the one given by first minimizing at fixed μ.

2. THE LANDAU EXPANSION

Under the assumption of infinite electron and hole lifetimes and neglecting magnetostrictive effects, the pairing Hamiltonian used for describing itinerant antiferromagnetism is equivalent to the following trial (mean-field, or Hartree-Fock) Hamiltonian:

$$H = \sum_{k,\sigma} [\epsilon_a(\vec{k}) a^+_{\vec{k}\sigma} a_{\vec{k}\sigma} + \epsilon_b(\vec{k}) b^+_{\vec{k}\sigma} b_{\vec{k}\sigma} + \epsilon_c(\vec{k}) c^+_{\vec{k}\sigma} c_{\vec{k}\sigma}] - \tag{2.1}$$

$$- \sum_{\vec{k},\vec{Q},\mu,\nu} [\Delta_{\vec{Q}} b^+_{\vec{k}+\vec{Q},\mu} (\vec{n}\vec{\sigma})_{\mu\nu} a_{\vec{k}\nu} + \text{h.c.}] + g^{-1} \sum_{\vec{Q}} |\Delta_{\vec{Q}}|^2 ,$$

where $\epsilon_{a,b,c}(\vec{k})$ are the energy spectra of bands a, b, c; a, b are the interacting bands with nearly nesting Fermi surfaces and c is the spectator band having the role of reservoir; $\Delta_{\vec{Q}}$ is the Fourier transform of the spatially modulated order parameter to be determined from the variational principle. We agree to take the origin of energies equal to the Fermi level corresponding to a half-filled band. Then, $\epsilon_a(\vec{k}) = -\epsilon_b(\vec{k}+\frac{1}{2}\vec{G})$ and the chemical potential μ has the meaning of half the difference between the Fermi levels in bands a and b.

We shall work in the usual approximations (T and μ much smaller than the band width). In particular, we take (cf., e.g., Ref.[1]) $\epsilon_a(\vec{k}) = \vec{v}(\vec{k}_F(\vec{k}))(\vec{k} - \vec{k}_F(\vec{k}))$, what amounts to an error of the order of μ/ϵ_F in the coefficients of q^2, q^4 in the Landau expansion.

The trial thermodynamic potential corresponding to the Hamiltonian (2.1) with the ansatz (1.1) for the order parameter is developed in powers of Δ up to sixth order:

$$N(0)^{-1} [\Omega(\mu, T; \Delta, \vec{q}, \cos\theta) - \Omega_{para}(\mu, T)] = \tag{2.2}$$

$$= A(\vec{q}, \cos\theta)\Delta^2 + \frac{1}{2} B(\vec{q}, \cos\theta)\Delta^4 + \frac{1}{3} C(\vec{q}, \cos\theta)\Delta^6 ,$$

where $N(0)$ is the total density of states in bands a and b, and

$$\Omega_{para}(\mu, T) = -2TN(0)(1+p) \int_{-w}^{w} d\epsilon \, \ell n[1 + \exp(\frac{\mu-\epsilon}{T})] \tag{2.3}$$

is the potential of the normal phase, with w a cut-off parameter and p the reservoir power ($pN(0)$ = the density of states in band c). The coefficients A, B, C are calculated in the usual way[14],[21],[1] and have the following expansion in powers of q up to the needed order:

$$A(\vec{q}, \cos\theta) = a - X\langle(\vec{v}\vec{q})^2\rangle/2(4\pi T)^2 + Y\langle(\vec{v}\vec{q})^4\rangle/4!(4\pi T)^4 , \tag{2.4a}$$

$$B(\vec{q}, \cos\theta) = -X(5 - \cos\theta)/4(4\pi T)^2 + Y\langle(\vec{v}\vec{q})^4\rangle(11 + \cos\theta)/4!(4\pi T)^4 , \tag{2.4b}$$

$$C(\vec{q}, \cos\theta) = Y(7 - 3\cos\theta)/16(4\pi T)^4 . \tag{2.4c}$$

Here, defining $\rho = \mu/2\pi T$ and denoting by T_0 the Néel temperature for $\mu = 0$, and by $\psi^{(n)}$ the n-th derivative of the digamma function, $\psi(z)$, one has:

$$a = \ell n(T/T_0) + \text{Re}[\psi(\tfrac{1}{2} + i\rho) - \psi(\tfrac{1}{2})] , \tag{2.5}$$

$$X = \text{Re}\psi^{(2)}(\tfrac{1}{2} + i\rho) , \tag{2.6}$$

$$Y = \text{Re}\psi^{(4)}(\tfrac{1}{2} + i\rho) . \tag{2.7}$$

It will be convenient to take

$$\xi^2 \equiv \langle(\vec{v}\vec{q})^2\rangle/2(4\pi T)^2 \tag{2.8}$$

as a new variational parameter, instead of q . Then, Eqs.(2.4) read as:

$$A(\vec{q}, \cos\theta) = a - X\xi^2 + dY\xi^4, \tag{2.9a}$$

$$B(\vec{q}, \cos\theta) = (4\pi T)^{-2}\,[-X(5-\cos\theta)/4 + Y\xi^2(11+\cos\theta)/12], \tag{2.9b}$$

$$C(\vec{q}, \cos\theta) = (4\pi T)^{-4}\, Y\,(7-3\cos\theta)/16, \tag{2.9c}$$

where the whole dependence on the shape of the Fermi surfaces is contained, within the accepted approximations, in the coefficient:

$$d = \langle(\vec{v}\,\vec{q})^4\rangle / 6\langle(\vec{v}\,\vec{q})^2\rangle^2 . \tag{2.10}$$

When taking $\vec{q}$ along one of the axes, one has $d = 3/10$ for spherical and $d = 1/6$ for octahedral Fermi surfaces.

3. CALCULATION OF THE GRAND-CANONICAL POTENTIAL

The grand-canonical potential of the model is defined as:

$$\Omega(\mu, T) = \min_{\Delta,\, \vec{q},\, \theta} \Omega(\mu, T; \Delta, \vec{q}, \cos\theta) \tag{3.1}$$

The triple point (μ^*, T^*) is defined by the equations:

$$a(\mu, T) = X(\mu, T) = 0. \tag{3.2}$$

We shall take (a , X) as new variables around the triple point.

The minimization over θ is immediate, as the coefficients (2.9) are linear functions of $\cos\theta$: the minimum is attained at one of the end points, $\cos\theta = \pm 1$. Hence, one can minimize over Δ and q the two functions $\Omega(\mu, T; \vec{q}, \pm 1)$ and take at the end the least of the two minima.

We consider first the region $X < 0$. Then, because the coefficients of ξ^2 , ξ^4 are positive, the minimum is attained at $\xi = 0$. Moreover, $\Omega(\mu, T; \Delta, 0, +1) \leq \Omega(\mu, T; \Delta, 0, -1)$. Hence, when $X < 0$, a second order phase transition P-CSDW occurs at $a = 0$.

When $X > 0$, it is convenient to look for the minimum at a , X fixed such that:

$$a = \lambda X^2 Y^{-1} \tag{3.3}$$

and to introduce the new variables:

$$Z = (4\pi T)^{-2}\,\Delta^2 Y X^{-1} \geq 0, \quad \zeta = \xi^2 Y X^{-1} \geq 0. \tag{3.4}$$

In terms of these, one is left with minimizing over $Z \geq 0, \zeta \geq 0$ the following functions:

$$N(0)^{-1}\,[\Omega(\mu, T; \Delta, \vec{q}, \pm 1) - \Omega_{para}(\mu, T)] = \tag{3.5}$$

$$= (4\pi T)^2 X^3 Y^{-2}\,[\lambda Z - a_\pm Z^2 + b_\pm Z^3 - Z\zeta(1 - c_\pm Z) + dZ\zeta^2],$$

where $a_\pm = (5\mp 1)/8$, $b_\pm = (7\mp 3)/48$, $c_\pm = (11\pm 1)/24$.
The minimum over ζ is attained at:

$$\zeta_\pm(Z) = \begin{cases} (2d)^{-1}\,(1 - c_\pm Z) & \text{if } Z < c_\pm^{-1} \\ 0 & \text{if } Z \geq c_\pm^{-1} \end{cases} . \tag{3.6}$$

Inserting these into Eq.(3.5), one is left with minimizing over $Z \geq 0$ the functions given by:

$$g_\pm(\lambda, d; Z) = \begin{cases} (4\pi T)^2 X^3 Y^{-2}\,[\lambda Z - a_\pm Z^2 + b_\pm Z^3], & \text{if } Z > c_\pm^{-1} \\ (4\pi T)^2 X^3 Y^{-2}\,[(\lambda - 1/4d)Z - (a_\pm - c_\pm/4d)Z^2 + (b_\pm - c_\pm^2/4d)Z^3], & \text{if } Z < c_\pm^{-1} \end{cases}$$

what is done straightforwardly. The minimum points, $Z_\pm$, obviously depend only on $\lambda = aYX^{-2}$, so the minimum values of $g_\pm$ themselves will be $(4\pi T)^2 X^3 Y^{-2}$ times some functions $f_\pm(\lambda, d) = g_\pm(\lambda, d; Z_\pm(\lambda))$. Hence, the minimum points themselves satisfy:

$$Z_\pm(\lambda) = \frac{d}{d\lambda} f_\pm(\lambda, d). \tag{3.7}$$

Finally, the needed minimum is obtained by comparing the two functions $f_\pm(\lambda, d)$, what is done numerically.

The final result of the analysis for $X > 0$ is (see also Fig.1):

$$\Omega(\mu, T) \equiv \min \Omega(\mu, T; \Delta, \vec{q}, \cos\theta) = \tag{3.8}$$

$$= \Omega_{para}(\mu, T) + N(0)(4\pi T)^2 X^3 Y^{-2}\, f(aYX^{-2}, d),$$

where

$$f(\lambda, d) = \begin{cases} 0 & \text{if } \lambda \geq \lambda_1(d) \\ f_-(\lambda, d) & \text{if } \lambda_1(d) \geq \lambda \geq \lambda_2(d) \\ f_+(\lambda, d) & \text{if } \lambda_2(d) \geq \lambda \end{cases} \tag{3.9}$$

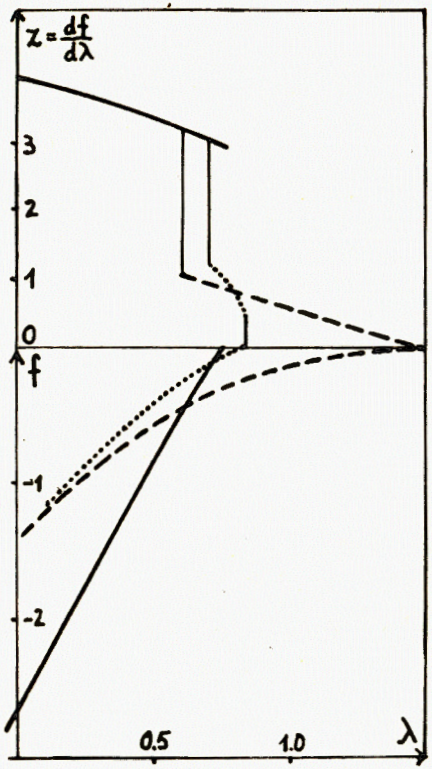

Fig.1. The graphs of $f(\lambda, d)$ and their derivatives for $d = 1/6$ and $d = 3/10$. Full curves are for f_+, broken for $f_-(\lambda, 1/6)$ and dotted for $f_-(\lambda, 3/10)$.

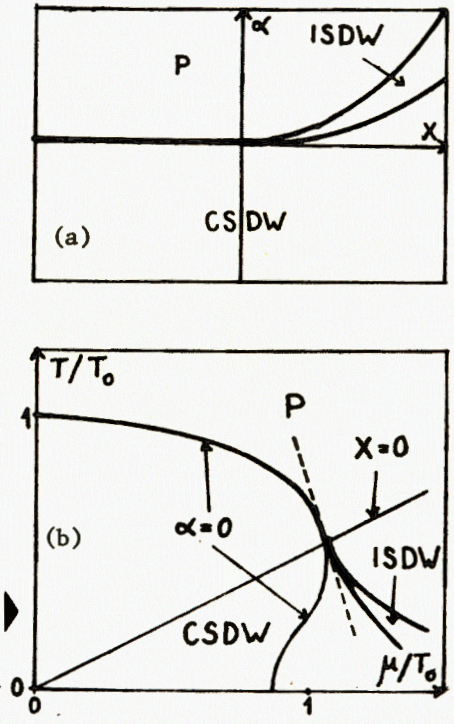

Fig.2. The phase diagram at fixed μ : a) in the variables (α, X) ; b) in the variables (μ, T). The broken line is the common tangent of the phase boundaries.

For all the values of d between 1/6 (octahedron model) and 3/10 (spherical model), for all αXY^{-2} between $\lambda_2(d)$ and $\lambda_1(d)$ the minimum is realised on a sinusoidal ISDW, while for all αYX^{-2} less than $\lambda_2(d)$ on the CSDW.

The order of the P-ISDW transition at $\lambda = \lambda_1(d)$ is controlled by the sign of $a_- - c_-/2d$: for $d \le c_-/2a_- = 5/18$ the transition is of 2nd order at $\lambda_1(d) = 1/4d$; for $d > 5/18$ the transition is of 1st order at $\lambda_1(d) = (1/4d) + \frac{1}{4}(a_- - c_-/2d)^2(b_- - c_-^2/4d)^{-1}$ and the jump of the order parameter is determined from:

$$Z_-(\lambda_1(d)) = \frac{1}{2}(a_- - c_-/2d)(b_- - c_-^2/4d)^{-1} . \qquad (3.10)$$

(In particular, $\lambda_1(3/10) = 93/110$ in agreement with Nakanishi and Maki [14]). On the other hand, the ISDW-CSDW transition at $\lambda_2(d)$ is of 1st order for all $1/6 \le d \le 3/10$; the actual values of $\lambda_2(d)$ and of the jump of Z are determinated numerically (e.g., $\lambda_2(3/10) \cong 0.71$, $\Delta Z(\lambda_2(3/10)) \cong 1.94$; $\lambda_2(1/6) \cong 0.61$, $\Delta Z(\lambda_2(1/6)) \cong 2.23$).

Thus, as far as the SDW states arise as bifurcations from the paramagnetic state, we have obtained the phase diagram around the triple point, Eq.(3.2), in the (α, X) variables: it consists of a P-CSDW 2nd order transition line ($\alpha = 0$, $X < 0$), a P-ISDW transition line ($\alpha = \lambda_1(d) X^2 Y^{-1}$, $X > 0$) whose order depends on d as said above, and a CSDW-ISDW 1st order transition line ($\alpha = \lambda_2(d) X^2 Y^{-1}$, $X > 0$), see Fig.2a. Its schematical representation in the (μ, T) plane is given in Fig.2b.

It is important to note that all transition lines meet with the same tangent at the triple point. Figure 2b, corresponding to an infinite reservoir power, does not resemble the experimental facts in that the P-ISDW transition is accompanied at a nearby temperature by an ISDW-CSDW transition (not observed for Cr) and on the other side of the triple point no CSDW-ISDW transition appears (though observed for Cr-Mn alloys of a concentration $\gtrsim 0.4\%$; see, for instance, Ref.[7]).

Moreover, the temperature dependence of q just below the Néel temperature near the triple point again contradicts the experiment [5,6], indeed, remembering Eqs.(3.4),(3.6):

$$\frac{\partial \xi^2}{\partial T}\Big|_{T = T_N(\mu)} = \frac{\partial X}{\partial T}(2dY)^{-1}(1 - c_-Z_-(\lambda_1(d))) - (2dY)^{-1} c_-f_-''(\lambda_1(d)) X \frac{\partial \lambda}{\partial T}$$

which becomes positive near the triple point ($XY^{-1} \to 0$), irrespective of the value of d, because $X\frac{\partial \lambda}{\partial T} \sim YX^{-1}\frac{\partial \alpha}{\partial T} \to \infty$, while $f_-''(\lambda_1) < 0$. (This had been already remarked by Nakanishi and Maki [14] in the special case of spherical Fermi surfaces)

4. CALCULATION OF THE HELMHOLTZ FREE ENERGY AND THE PHASE DIAGRAM

The change from the (μ, T)-variables to the physically interesting (n, T)-variables (where n is the electron density) is to be performed, according thermodynamics, via the Legendre transformation, which expresses the Helmholtz free energy, $F(n, T)$, in terms of $\Omega(\mu, T)$ as [20] :

$$F(n, T) = \sup_{\mu} [\Omega(\mu, T) + \mu n]. \qquad (4.1)$$

The thermodynamics of the model in the (n, T)-variables is fully specified by Eqs.(3.8),(3.9) and (4.1). It should be mentioned that, while in $\Omega(\mu, T)$ the reservoir power p enters additively through $\Omega_{para}(\mu, T)$ (see Eq.(2.3)), this is not the case for $F(n, T)$ due to the Legendre transformation.

Following Rice [11] we shall use instead of n the variable:

$$\mu_p = (1+p)^{-1} N(0)^{-1} n - w \qquad (4.2)$$

which is linearly related to n. Cf.Eq.(2.3):

$$-\frac{\partial \Omega_{para}}{\partial \mu} = N(0)(1+p) \int_{-w}^{w} d\epsilon \, \frac{1}{2}\left(1 + \tanh \frac{\mu - \epsilon}{T}\right) = \qquad (4.3)$$

$$= N(0)(1+p)(\mu + w + O(\exp(-w/2T))).$$

So μ_p has, up to corrections negligibly small in the interesting temperature range, the meaning of chemical potential in the absence of interactions.

We want to construct the phase diagram in the (μ_p, T)-plane. To this aim, remark first that the paramagnetic region will be the same as in the (μ, T)-diagram and that by symmetry $\mu = 0$ goes into $\mu_p = 0$. Second, because outside the 1st order transition lines $\Omega(\mu, T)$ is differentiable, every point (μ, T) there goes into a point (μ_p, T), where

$$\mu - \mu_p = (1+p)^{-1} \frac{\partial}{\partial \mu} N(0)^{-1} [\Omega(\mu, T) - \Omega_{para}(\mu, T)] = \qquad (4.4)$$

$$= (1+p)^{-1} (4\pi T)^2 \frac{\partial}{\partial \mu} [Y^{-2} X^3 f(\alpha Y X^{-2}, d)],$$

while $F(\mu_p, T)$ is obtained by inserting the solution μ of Eq.(4.4) into $\Omega(\mu, T) + \mu N(0)(1+p)(\mu_p + w)$.

Let $\mu = \phi_\lambda(T)$ be the curve determined by the equation $\alpha Y X^{-2} = \lambda$ ($\lambda \neq \lambda_1(d), \lambda_2(d)$), and $\mu_p = \psi_\lambda(T)$ be its image through Eq.(4.4). Then, the tangent of $\mu_p = \psi_\lambda(T)$ at the triple point is given by:

$$\frac{d\psi_\lambda}{dT} = \frac{d\phi_\lambda}{dT} - (1+p)^{-1} (4\pi T)^2 Y^{-1} \frac{\partial \alpha}{\partial \mu}\left(\frac{\partial X}{\partial \mu}\frac{d\phi_\lambda}{dT} + \frac{\partial X}{\partial T}\right) f'(\lambda, d) \cong \qquad (4.5)$$

$$\cong -0.311 + 3.448 (1+p)^{-1} f'(\lambda, d).$$

(Here all functions are evaluated at the triple point).

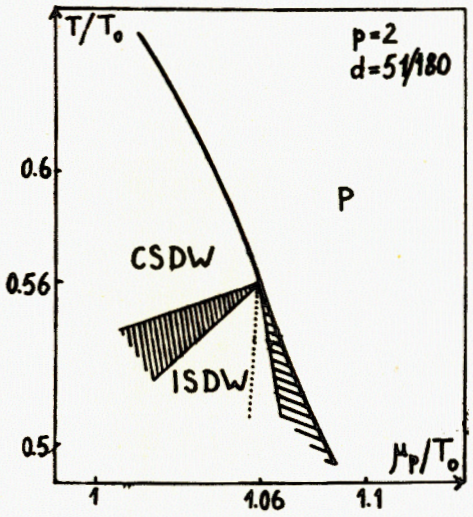

Fig.3. The phase diagram at fixed electron density to leading order around the triple point ($p=2$, $d=51/180$). The dotted line is the right boundary of the pure ISDW phase for $d=3/10$. Shaded regions correspond to phase mixtures.

However, at $\lambda = \lambda_i(d)$, $f(\lambda, d)$ is not differentiable if either $i = 2$, or $i = 1$, $d > 5/18$, and in these cases:

$$\psi^{-}_{\lambda_i(d)}(T) \equiv \lim_{\lambda \to \lambda_i(d) - 0} \psi_\lambda(T) < \psi^{+}_{\lambda_i(d)}(T) \equiv \lim_{\lambda \to \lambda_i(d) + 0} \psi_\lambda(T).$$

One point, $(\phi_{\lambda_i(d)}(T), T)$ of the (μ, T)-diagram goes into the horizontal segment $\{(\mu_p, T) : \psi^{-}_{\lambda_i(d)}(T) \leq \mu_p \leq \psi^{+}_{\lambda_i(d)}(T)\}$, , on which phases coexist and $F(\mu_p, T)$ interpolates linearly between its values at the ends of the segment. The tangents at the triple point of the boundaries, $\mu_p = \psi^{\pm}_{\lambda_i(d)}(T)$, of the pure phases are given by Eq.(4.5) with f' replaced by the corresponding left or right derivative. (These are represented in Fig.3 for $p = 2$, which seems adequate for Cr alloys, and $d = 51/180 > 5/18$). In view of Eq.(3.10), $f'_{-}(\lambda_1(d), d)$ is a decreasing function of d, hence when d increases from 5/18 to 3/10, the tangent of $\mu_p = \psi^{-}_{\lambda_i(d)}(T)$ rotates from the tangent of $\mu_p = \psi^{+}_{\lambda_i(d)}(T)$ (which is independent of d) to its position in the unequal sphere model (the latter is shown as a dashed line in Fig.3). On the other hand, as $f'_{\pm}(\lambda_2(d), d)$ are slowly varying with d in the considered range, the position and width of the mixed CSDW-ISDW region do not change considerably.

5. THE TEMPERATURE DEPENDENCE OF THE WAVE VECTOR OF THE SDW

We shall next consider the temperature dependence of q with lowering temperature below the Neel temperature at fixed μ_p (corresponding to a given concentration of the Cr-Mn, V alloy).

Remembering Eqs.(2.8),(3.4),(3.6),(3.7) and that q is along the x axis, one has:

$$q(T)^2 = \xi(T)^2 \cdot 2(4\pi T)^2 / \langle v_x^2 \rangle = XY^{-1}[1 - c\_f'\_(\lambda, d)](4\pi T)^2 / d \cdot \langle v_x^2 \rangle , \quad (5.1)$$

where X, Y, λ are to be calculated at the point $(\mu(T), T)$, whose image through the Legendre transformation is (μ_p, T).. Differentiating Eq.(5.1) (at fixed μ_p), one obtains to the leading order:

$$d \cdot \langle v_x^2 \rangle \cdot \frac{dq(T)^2}{dT} = (4\pi T)^2 \frac{dX}{dT} Y^{-1}[1 - c\_f'\_(\lambda, d)] - \quad (5.2)$$

$$- (4\pi T)^2 c\_ XY^{-1} f''\_(\lambda, d)\frac{d\lambda}{dT} ,$$

where the values of $\frac{dX}{dT}$, Y are taken at the triple point.

When (μ_p, T) is inside the region of the mixed P-ISDW states, clearly $\lambda = \lambda_1(d)$ (i.e., does not depend on temperature), hence:

$$d \cdot \langle v_x^2 \rangle \frac{dq(T)^2}{dT}\Big|_{mixed} = (4\pi T)^2 \frac{dX}{dT} \cdot Y^{-1}[1 - c\_f'\_(\lambda_1(d), d)]. \quad (5.3)$$

When (μ_p, T) is inside the pure ISDW region, $\mu(T)$ is the solution of Eq.(4.4). Differentiating Eq.(4.4) (at fixed μ_p) and taking into account:

$$\frac{d\lambda}{dT} = \frac{\partial\lambda}{\partial\mu} \cdot \frac{d\mu}{dT} + \frac{\partial\lambda}{\partial T}$$

and Eq.(4.5), one obtains to the leading order:

$$- f''\_(\lambda, d) X \frac{d\lambda}{dT} = (1 + p) Y \frac{\partial a}{\partial T} / (4\pi T)^2 (\frac{\partial a}{\partial \mu})^2 + f'\_(\lambda, d)\frac{dY}{dT} = \quad (5.4)$$

$$= - [(1 + p) Y / \frac{\partial a}{\partial \mu} (4\pi T)^2] \cdot \frac{d\psi_\lambda}{dT} .$$

Inserting Eqs.(5.4) into (5.2) one obtains the following two alternative formulae for $\frac{dq(T)^2}{dT}$ in the pure ISDW phase:

$$d \cdot \langle v_x^2 \rangle \frac{dq(T)^2}{dT}\Big|_{pure} = (4\pi T)^2 Y^{-1} \frac{dX}{dT} + c\_ (1 + p)\frac{\partial a}{\partial T} / (\frac{\partial a}{\partial \mu})^2 =$$

$$= d \cdot \langle v_x^2 \rangle \frac{dq(T)^2}{dT}\Big|_{mixed} = - [(1 + p) c\_ / \frac{\partial a}{\partial \mu}] \cdot \frac{d\psi_\lambda}{dT} . \quad (5.5)$$

Since $\frac{dX}{dT} = - T^{-1} \cdot 15.448 < 0$, Eq.(5.3) shows that $\frac{dq(T)^2}{dT}|_{mixed}$ is always negative irrespective of the values of p and d. As the pure ISDW is never reached along lines $\mu_p = \text{const} > \mu^*$ unless $\frac{d\psi_\lambda}{dT} < 0$, it follows from Eq.(5.5) that

$$- \frac{dq(T)^2}{dT}\Big|_{mixed} > - \frac{dq(T)^2}{dT}\Big|_{pure} .$$

Moreover, from the first Eq.(5.5), $d \cdot \langle v_x^2 \rangle \frac{dq(T)^2}{dT}|_{pure}$ does not depend on d and is negative for:

$$p < [(4\pi T)^2 \frac{dX}{dT} \cdot (\frac{\partial a}{\partial \mu})^2 / Y c\_ \frac{\partial a}{\partial T}] - 1 \cong 25.648.$$

The numerical values for $d = 51/180$ and $p = 2$ are:

$$- [d \cdot \langle v_x^2 \rangle / (4\pi)^2 T] \frac{dq(T)^2}{dT} = \begin{cases} 0.0458 \text{ in the P-ISDW mixed phase} \\ 0.0449 \text{ in the pure ISDW phase,} \end{cases}$$

what shows that $\frac{dq(T)^2}{dT}$ is almost the same in the pure and mixed ISDW phases.

Summing up, irrespective of the shape of the Fermi surface (in particular, of the order of the P-ISDW transition), and for μ_p near its value μ^* at the triple point, q has a T-dependence in agreement with experiment for all $T < T_N$.

REFERENCES

1. Buker D.W. Phys.Rev., 1981, B24, p.991.
2. Arrott A., Werner S.A., Kendrick H. Phys.Rev.Lett., 1965, 14, p.1022.
3. Garnier P.R., Salamon M.B. Phys.Rev.Lett., 1971, 27, p.1523.
4. Benediktsson G., Aström H.U., Rao K.U. J.Phys.F: Met.Phys., 1975, 5, p.1966.
5. Werner S.A., Arrott A., Kendrick H. Phys.Rev., 1967, 155, p.528.
6. Umebyashi H., Shirane G., Frazer B.C., Daniels W.B. J.Phys. Soc. Japan, 1968, 24, p.368.
7. Geerken B.M. et al. J.Phys.F: Met.Phys., 1982, 12, p.1603.
8. Overhauser A.W. Phys.Rev., 1962, 128, p.1437.
9. Lomer W.H. Proc.Phys.Soc., 1962, 80, p.489.
10. Shibatani A., Motizuki K., Nagamiya T. Phys.Rev., 1969, 177, p.984.
11. Rice T.M. Phys.Rev., 1970, B2, p.3619.
12. Keldysh L.V., Kopaev Yu.V. Fiz.Tverd. Tela, 1964, 6, p.2791.

13. Malaspinas A., Rice T.M. Phys.Kondens. Materie, 1971, 13, p.193.
14. Nakanishi R., Maki R. Progr.Theor.Phys., 1972, 48, p.1059.
15. Sato H., Maki R. Int.J. Magnetism, 1974, 6, 183.
16. Kotani A. J.Phys.Soc. Japan, 1975, 39, p.851.
17. Fenton E.W. J.Phys.F: Met.Phys., 1976, 6, p.2403.
18. Angelescu N., Nenciu G., Tonchev N.S. JINR, E17-82-798, Dubna, 1982.
19. Angelescu N., Nenciu G., Tonchev N.S. Phys.Lett., 1983, 93A, p.201.
20. Griffiths R.B. Phase Transitions and Critical Phenomena, vol.1, eds. Domb C., Green M.S., Academic Press, New York, 1972, pp.33-37.
21. Kasuya T., Nakanishi K. J.Phys.Soc. Japan, 1977, 42, p.833.

Received by Publishing Department
on April 23, 1983.

SUBJECT CATEGORIES OF THE JINR PUBLICATIONS

Index	Subject
1.	High energy experimental physics
2.	High energy theoretical physics
3.	Low energy experimental physics
4.	Low energy theoretical physics
5.	Mathematics
6.	Nuclear spectroscopy and radiochemistry
7.	Heavy ion physics
8.	Cryogenics
9.	Accelerators
10.	Automatization of data processing
11.	Computing mathematics and technique
12.	Chemistry
13.	Experimental techniques and methods
14.	Solid state physics. Liquids
15.	Experimental physics of nuclear reactions at low energies
16.	Health physics. Shieldings
17.	Theory of condenced matter
18.	Applied researches
19.	Biophysics

Ангелеску Н., Ненчу Г., Тончев Н.С. E17-83-284

О влиянии резервуара и формы поверхности Ферми
на фазовую диаграмму двухзонных моделей для сплавов Cr

Для класса моделей, включающего модель Райса и модель Шибатани и др., исследовано разложение Ландау в окрестности тройной точки. Показано, что при корректном учете влияния резервуара для реалистических значений параметров модели можно получить фазовую диаграмму, которая согласуется с экспериментом. Получен "узкий" фазовый переход из парамагнитного в несоизмеримое антиферромагнитное состояние (для чистого Cr) и фазовый переход второго рода из парамагнитного в соизмеримое антиферромагнитное состояние (для сплавов Cr с большой концентрацией Mn). В последнем случае при понижении температуры имеет место еще один фазовый переход первого рода из соизмеримого в несоизмеримое состояние. Для вектора несоизмеримости получена температурная зависимость, которая качественно согласуется с экспериментом.

Работа выполнена в Лаборатории теоретической физики ОИЯИ.

Препринт Объединенного института ядерных исследований. Дубна 1983

Angelescu N., Nenciu G., Tonchev N.S. E17-83-284

On the Influence of the Reservoir and of the Shape of the Fermi
Surface on the Phase Diagram of the Two-Band Models for Cr Alloys

The Landau expansion around the triple point for a class of mean field two band models including Rice's unequal sphere model and the octahedron model of Shibatani et al., is studied within the infinite lifetime approximation and neglecting magnetostriction. It is shown that, when correctly taking into consideration the reservoir, one can obtain with reasonable values of the parameters a phase diagram in agreement with experiment, i.e., a narrow first order transition from paramagnetic to an incommensurate antiferromagnetic phase for nearly pure Cr and second order paramagnetic to commensurate phase transition accompanied at a lower temperature by a wide 1st order commensurate-incommensurate transition for Mn-rich Cr alloys. The temperature dependence of the wave vector in the incommensurate phase is shown to be in qualitative agreement with experiment, as well.

The investigation has been performed at the Laboratory of Theoretical Physics, JINR.

Preprint of the Joint Institute for Nuclear Research. Dubna 1983